

Structural aspects of cold-formed steel section designed as U-shape composite beam

Cite as: AIP Conference Proceedings **1903**, 020025 (2017); <https://doi.org/10.1063/1.5011505>
Published Online: 14 November 2017

Anis Saggaff, Mahmood Md. Tahir, Mohammadamin Azimi, and T. M. Alhajri



View Online



Export Citation

ARTICLES YOU MAY BE INTERESTED IN

[Finite element analysis of composite beam-to-column connection with cold-formed steel section](#)

AIP Conference Proceedings **1903**, 020024 (2017); <https://doi.org/10.1063/1.5011504>

[Prediction on flexural strength of encased composite beam with cold-formed steel section](#)

AIP Conference Proceedings **1903**, 020016 (2017); <https://doi.org/10.1063/1.5011496>

[Experimental behaviour of beam-column connection using cold-formed steel sections with rectangular gusset-plate](#)

AIP Conference Proceedings **1903**, 020006 (2017); <https://doi.org/10.1063/1.5011486>

Lock-in Amplifiers
up to 600 MHz



Structural Aspects of Cold-Formed Steel Section Designed as U-Shape Composite Beam

Anis Saggaff^{1, a)}, Mahmood Md. Tahir^{2, b)}, Mohammadamin Azimi^{2, c)}, and T. M. Alhajri^{2, d)}

¹*Professor, Structure and Construction Research Laboratory (SCRL), Civil Engineering Department, Universitas Sriwijaya, Indralaya - OI, Sumatera Selatan 30662, Indonesia.*

²*Institute for Smart Infrastructure and Innovative Construction (ISIIC), UTM Construction Research Centre, Faculty of Civil Engineering, Universiti, Teknologi Malaysia (UTM), 81310 Johor Bahru, Johor, Malaysia.*

^{a)}anissaggaff@yahoo.com

^{b)}Corresponding author: mahmoodtahir@utm.my

^{c)}mohammadamin@utm.my

^{d)}t-alfahed@hotmail.com

Abstract. Composite beam construction usually associated with old-style Hot-Rolled Steel Section (HRSS) has proven to act much better in compare with Cold-Formed Steel Section (CFSS) sections due to thicker section. Due, it's getting popular to replace HRSS with CFSS in some aspects as a composite beam. The advantages such as lightweight, cost effective and easy to install have contributed to the apply CFSS as a preferred construction material for composite beam. There is a few technical data available regarding the application of the usage of CFSS as a composite system, despite the potentials use for residential and light-weight industrial constructions. This paper presents an experimental tests results which have been conducted using CFSS as composite beam. Composite action of CFSS arranged as double beam with Self-Compacting Concrete (SCC) slab are integrated together with bolted shear connectors were used. A full-scale test comprised of 3 proposed composite beam specimens with bolted shear connector spaced at 300 mm interval of grade 8.8 was using single nut with washer on flange of CFS, cast to the slab and loaded until failed. The test show that the bolted shear connector yielded better capacity of ultimate strength and ultimate moment for the proposed composite beam. It can be concluded that, bolted shear connectors of 16 mm in diameter performed better than the other diameter size of bolted shear connectors.

INTRODUCTION

Composite construction has been well known in current decades and has largely applied in steel frames construction in many develop countries. The main structural benefits in using composite beams can be listed as follows: [1]

1. Generally reduce steel weight up to 30 to 50% than the hot-rolled section one.
2. The higher composite beams stiffness mean can shallower the beam deck for the same span, lowering the story heights and reduce cladding cost.
3. Faster in speed of construction and reduce the usage of form work

Thickness of Cold-formed Steel (CFS) ranging from 1.2 mm to 3.2 mm [2], would be as a sustainable and green material as especially for low rise building in developing country. Current researches on CFS as a composite beam already done by many researchers and also had been applied [3]. Although to be found, lack of data and information on CFS performance. Its application is limit for roof trusses system and non-structural elements [4-6]. Thickness has been found as one of the limitations of CFS, especially section thinness prone to local buckling, torsion, distortion;

lateral torsion and lateral distortion. Therefore, an effective solution can be resorting to structural CFS section composite construction as well as reinforced concrete slab. This reduces the depth from the top of the deck to neutral-axis and also decreases bending stress of the CFS sections. Moreover, using back-to-back, the web of CFS sections will avoid buckling and distortion. Old version of composite beam normally consists of concrete slab and hot rolled beam. Its analyzing based on mechanism of shear transfer from shear connectors. Hence, shear connectors design and execution is important for providing optimum capacity of connection and also its ductility.

Previous Research Works

Generally, it is not economical using hot rolled beam for small and medium size of structures due to waste materials, fabricating cost, erection, and labor cost. Furthermore, general application of CFS elements currently is only for non-composite members design and resulting the larger size in application. Thus, for the economic reasons it used CSF replacing the hot rolled section for small and medium size of structures, and by combining a concrete slab become a composite member. Therefore, by using CFS section can reduce its waste material and labor cost as mention above.

In the year of 2000, Hanaor investigate d the composite action of concrete slab and cold formed steel I-sections by using two different shear connector types. The first type is using two different method of welding of lip channel and the second type is using self-drilling screws.

This shear connector used vertical webs and to be connected using self-drilling screws. The connectors use for resisting the longitudinal shear by using their end bearing as same as with the channel shear connectors for hot rolled steel-concrete slabs. Sufficient resistance against uplift forces can be provided by the lips of shear connectors. Results showed the higher performance and capacity of welded channel connectors in comparison with self-drilling screws. Better connection can be provided as well as shear connector's flange by welding. Therefore, the specimen failure was first started by steel section buckling and after that by welding failure and concrete crushing. It can be realized that the screws themselves are the weakness part in screwed shear connectors. When loading is increased, at ultimate load, tilting of the screws existed and pulling-out or shear off with buckling of the deck for the second type.

Composite light steel beam comprises steel decking, double C-cold formed steel sections, concrete slab with mesh reinforcement and profiled strip shear connector [1]. The profiled strip shear connectors were fastened to the top steel beam flange through the steel decking using 2 powder actuated pins per deck rib. Push-out test was conducted for specimens with strip shear connector to determine the ductility and strength of the shear connector. In addition, full-scale test beam was conducted. Double 425 mm cold formed steel sections of 3mm thickness and 280 MPa yield strength, concrete slab of 110 mm thickness and 2.4 m width with perpendicular steel decking and strip shear connectors were formed the light composite beam of 9.3 m span. The results showed that the failure was occurred at 68 mm deflection and moment capacity of 312 kN.m which is 188 % higher than moment capacity of double cold formed steel beam. The failure was due to the longitudinal shear resulting in rotation of actuated pins. It was observed that the design and measured moment capacities of the composite beam have very good agreement with ratio of 1.013. Thus, it could be concluded that the plastic resistance of the composite beam is developed. It should be mentioned that the light composite beam Training Centre at Ashorne Hill, Warwickshire.

In year 2006 Lakkavalli and Yi Liu investigated the composite slab joists performance including cold formed steel C-sections and concrete. They studied the shear transfer mechanisms, including pre-drilled holes, surface bond and self-drilling screws. Different types of shear connector's mechanisms were applied on the flange surface embedded inside the concrete. The surface bond was the first mechanism where the longitudinal shear force is considered to be transferred by shear and friction resistance of concrete and flange surface of steel beam. This mechanism is normally too weak. So, the surface bonding to develop composite by profiled steel sheeting is ignored. The pre-fabricated bent-up tabs is the second mechanism that avoids the longitudinal shear force with end bearing resistance. The third mechanism known as pre-drilled holes shear transfer that the concrete dowels formed over the pre-drilled holes resist the longitudinal shear force. The self-drilling screws is the last applied mechanism. The screw resists the longitudinal shear forces in a same method as welded stud shear connector. The thickness effect of cold formed C-sections on the composite slab joists capacity was studied by applying two various thicknesses including 1.905 and 1.524 mm. The results indicated that the pre-fabricated bent-up tabs shear connectors experienced the highest performance after that drilled holes in the embedded flanges and self-drilling screws.

FULL-SCALE TEST

The connections are normally designed as pinned joint at the structural steel elements that the beam is basically designed as a simple beam. Thus, simple composite beam full-scale testing was setting up. Full-scale tests aim to estimate and evaluate the performance of the proposed concrete slab and CFSS. The length of specimens were tested by using simple beam was 4,200 mm with four-point load system. Two points load subject to the beam at 1,400 mm apart from the supports as shown in Fig. 1. This loading system yielded a constant bending moment between the point loads. Therefore, the proposed composite ultimate flexural capacity can be determined.

Test Specimens

Total specimens for full scale tests were 13 composite beams and summarized in Table 1. The length of the beams was 4,500 mm and the span between supports was 4,200 mm for all of the proposed composite beam. The mechanism of test such a way that the beams fail due to flexural. ENERPAC-Universal Testing Machine with 1,000 kN capacity of load cell to be used. The actual length of the beam was 4,500 mm. However, an excess of 150 mm of each end from the beam was purposely done to ensure that the beam was simply supported with an effective length of 4,200 mm.

The concrete slab width was 1,500 mm and the thickness was 50 mm for specimen proposed in first nine specimens and 75mm for specimens proposed in last four specimens. The I-section was constructed using CFS beam can be shown at Figure 1 and 12 mm, 14 mm. and 16 mm bolts in last four specimens. Two nuts were used to fix the bolt. The first one was installed inside and the second one was installed outside the CFS section top flange surface. The top flange of CFS section holds with the two nuts. The wire mesh with spacing of 80 mm x 80 mm and diameter bar of 5 mm were applied between 2, 4, and 6 wire mesh layer (1.2 mm diameter). Wire mesh application in the slab has revealed higher capacity and flexural stiffness according to the work done by Richard et. Al [7]. Fig.2 present the layout test specimen.

The casting of slabs for all composite beams utilized the similar mortar batch. This was to ensure that the mortar properties remained same in all beams. For supporting the tested specimens, a pin and a roller was used to specify that the test was simple beam condition. Steel section bottom flange deflections were observed at the center-points and quarter-points by LVDT [8-11]. A bubble level was used to level up the transducers in order to read the best possible vertical displacements. Transducer was measured slip that was attached at the slab top side and the slab cross section centreline. Slip was measured in various deformations of the two elements, between slab and CFS. The installation of strain gauges were in the mid-span section of the bottom and top flanges of CFS beam as well as top surface of concrete slab. Fig. 1 displays the arrangement of strain gauges and transducers. Strain gauges were applied in concrete to record the compressive and tensile strain and installed longitudinally in the span direction to monitor the longitudinal (flexural) stresses. The setting up of the test is shown in Fig. 3.

TABLE 1. Full-scale test specimens detailing

Specimen	Shear connectors type	Length (L) mm	CFS thickness (t_c) mm	Spacing of shear connector (mm)
FS1	Bolt 12	4200	2	150
FS2	Bolt 12	4200	2	150
FS3	Bolt 12	4200	2	150
FS4	Bolt 12	4200	3	150
FS5	Bolt 12	4200	3	150
FS6	Bolt 12	4200	3	150
FS7	Bolt 12	4200	4	150
FS8	Bolt 12	4200	4	150
FS9	Bolt 12	4200	4	150
FS10	Bolt 14	4500	2.3	300
FS11	Bolt 14	4500	2.3	250
FS12	Bolt 12	4500	2.3	300
FS13	Bolt 12	4500	2.3	250

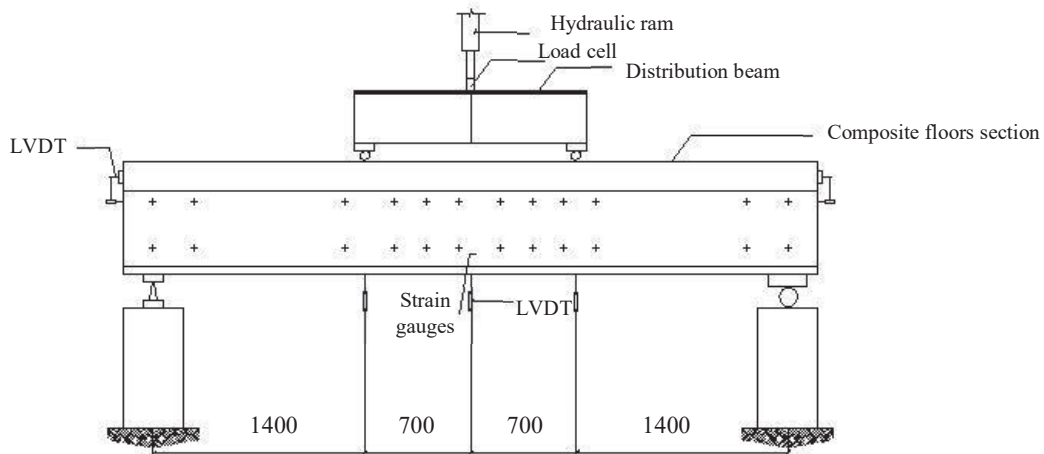


FIGURE 1. Arrangement of strain gauges and transducer for full scale test (All dimensions in mm)

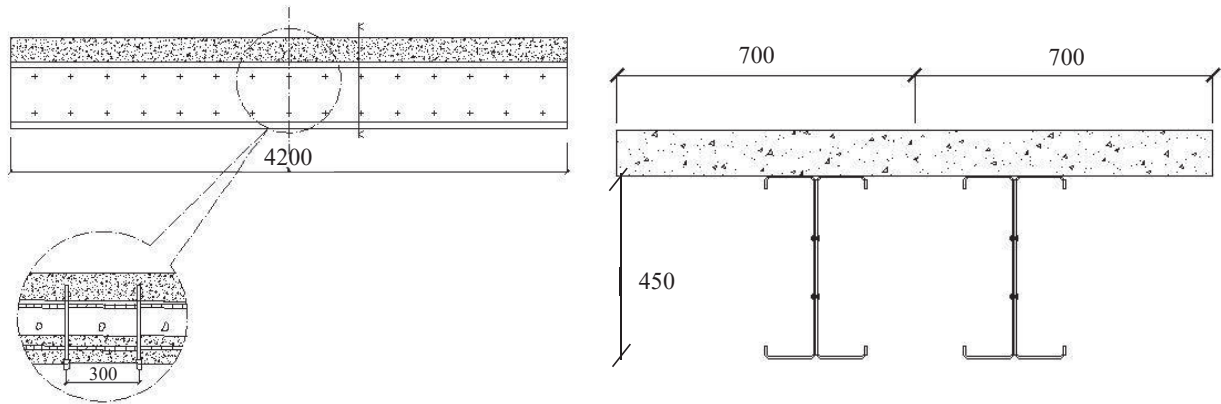


FIGURE 2. Concrete slab and CSF beam specimen – lay-out

Test Procedures

The load was applied to the top of the slab using jack of 1,000 kN jack capacity. All loads from the jack were distributed to two points spacing at 1,400 mm apart on the test specimen as shown in Fig. 1. The distance was taken to represent a pure bending moment developed at the mid-section of the specimen. Later the instrumentation system was set-up and the specimen had been installed in the test rig, data collection software was applied for checking the measurements of all connected channels to the instruments [12-15]. For calibration and gauge factors from manufacturer, correction factors are inserted into the software before to each test. Then load was applied up to one-third of the expected value. The load recording was done as point load because of easier controlling. Finally, when reach the one-third of expected load capacity, the load was released back. This approach was conducted to make the specimen to be in the equilibrium state prior to the actual test. The increasing of 5 kN was assumed so that a uniform data and normal specimen failure was recorded. Furthermore, the specimen was loaded again; though, the used load was not limited to the one-third capacity. As an alternative, the specimen was more loaded till large deflection of the beam can be detected. In this level, the loading arrangement was controlled by the increasing the deflection as a small load increasing due to large deflection incrimination. Hence, the load was applied but each step of the loading was restricted to the deflection of 5 mm of the beam. This process was sustained till the failure condition of the specimen which is an abrupt or large decreasing of the used load or when a large deformation.

In preventing pre-mature failures, several precautions were taken into consideration. The first precaution was to restrain the beam specimen laterally at both ends of the beam so as to prevent lateral buckling of the CFS section

during loading as shown in Fig. 4. Steel plates and restraints were provided between beams and reaction points to reduce the possibility of lateral buckling. Though, for allowing the beam vertical displacement, rollers was applied to the restraint. It was meant to avoid any web local failure because of concentrated load.



FIGURE 3. Instrumentation setup



FIGURE 4. Lateral restraint

Material Properties

All the material to be tested under ASTM relating standard [16, 17, and 18]. E.g. compressive strength, splitting strength of Self Compacting Concrete, yield strength and ultimate strength of cold-form. The grade, diameter, and length of bolt to be used in this study were 8.8, 12 mm and 70 mm respectively. The test result if the materials were show in Table 2.

TABLE 2. Material's tested data

CFS Thickness, t (mm)	Yield strength, F_y (N/mm ²)	Ultimate tensile strength, F_u (N/mm ²)	E_s (MPa)
2	326.4	424.9	194016.2
2.3	329.6	426.8	198122.4
3	331.3	430.7	201118.3
4	329.7	429.0	198136.2
Wire mesh , t (mm)			
1.2	418	522.7	202894.6
5	680	705	210223.6
Bolt, t (mm)			
12	704.3	906.3	202456

RESULTS AND DISCUSSION

Failure Mechanisms

The two failure mode of the full-scaled test can be seen in the Table 3.

TABLE 3. Failure mechanisms

Failure Mode	Description
1	Ferrocement crushed
2	Local buckling–CFS

Load versus mid-span deflection graphs was given in Fig.5. Based on Table 3 and Fig. 6, the ultimate load P_u of specimen FS1, FS2, and FS3 with 2mm thickness of CFS were 188.5 kN, 191.9 kN and 194.4 kN, respectively. At ultimate loads, mid-span deflections of 137.6 mm, 136.2 mm and 133.7 mm were recorded for Specimen FS1, FS2 and FS3, respectively. From the test result, especially in elastic range, can be explain there were a linear correlation increasing of mid-span deflection versus load for all specimen. The failure of these three specimens investigated due to flexural failure. Generally, the first cracks were formed below the tip of the load. Crack at the ferrocement slabs were first observed at a load of 110 kN for specimen FS1, 138 kN for specimen FS2 and 168 kN for specimen FS3. It is good to mentioned that in these three tested specimens, failure was due to ferrocement crushing with yielding steel as shows in Fig. 7.

In FS4, FS5 and FS6 specimens with CFS thickness of 3 mm, failure was due to the ferrocement crushing. The cracking pattern at failure is shown in Fig. 8. For all specimens of FS4, FS5 and FS6, the first crack occurred underneath the loading position at load 145.4 kN, 152.3 and 161.7 kN for specimens FS4, FS5 and FS6, respectively. The ultimate loads, P_u of specimens FS4, FS5 and FS6 are 346.2 kN, 361.3 and 364.1 kN, respectively. The corresponding mid-span deflections were recorded as 122.1 mm, 110.9 mm and 92.4 mm for specimens FS4, FS5 and FS6, respectively.

FS7, FS8 and FS9 are specimens with CFS thickness of 4 mm. This three specimens displayed better resistance than previous 6 specimens. It was observed that first transverse crack was observed at load of 164 kN, 171.4 kN and 184 kN for FS7, FS8 and FS9, respectively, through the part of the ferrocement slab underneath the point loads. The crack started from the top surface of the ferrocement slab under the point load as shown in Figure 7. This crack generally extended across the slab and become wider as the ultimate load was reached. Longitudinal cracks located at the center and extended along the ferrocement slab length was appeared at load and become wider as load increases. Transverse cracks formed at the specimen's shear span were detected immediately before ultimate load at the failure. All specimens were failed by the ferrocement crushing.

FS10 and FS11 are two specimens with CFS thickness of 2.3 mm and bolt of 14. As it can be observed from Fig. 6, the ultimate loads attained for specimens FS10 and FS11 were 440.6 kN and 472.1 kN respectively. Mid-span deflections at ultimate loads level were recorded as 49.7 mm and 54.94 mm for FS10 and FS11 specimens respectively. However, at elastic condition, as the load increased, linear increment of mid-span deflection was observed. Failure mode experienced by the specimens was appearance of a longitudinal cracks along the shear connectors' line on the concrete slab surface and transverse cracks underneath the slab. CFS web buckling was also observed along the span of the specimens on the CFS section when the ultimate load was reached.

FS12 and FS13 specimens have CFS thickness of 2.3mm and bolt 12. The ultimate loads of specimens FS12 and FS13 were 438.5 kN and 466.1 kN respectively, and the corresponding mid-span deflections recorded at ultimate loads level were 49.62 mm and 56.93 mm for FS12 and FS13 specimens respectively. The specimens in this category exhibited similar mode of failure. The failure mode initiated was formation of longitudinal cracks along line of shear connectors on surface of concrete slab. Transverse cracks were observed under the concrete slab and shear connector was pulled-out from the slab that could be recognized to the same head diameter of the shear connector. This is obvious, because, as the head diameter of the shear connector is small, there is a tendency of pull-out of the connector from the concrete slab as the resistance of the connector to pull-out force is relatively small.

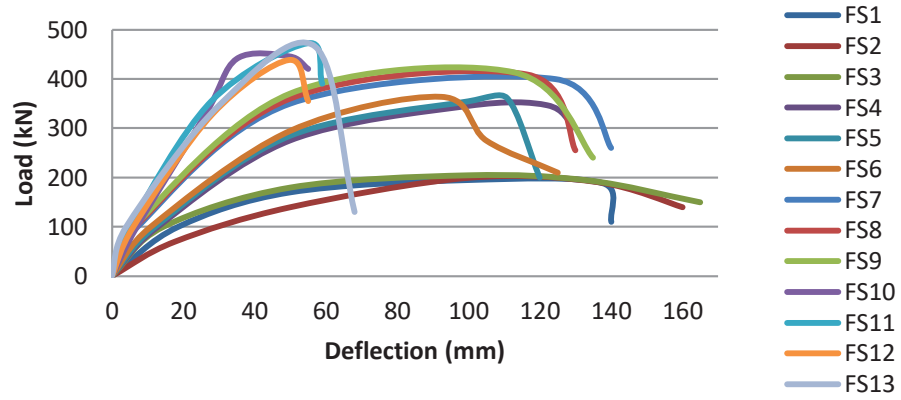


FIGURE 5. Load-deflection curves for all tested specimens



FIGURE 6. Buckling of steel beam flange, CFS thickness 2mm



FIGURE 7. Longitudinal crack, CFS thickness 3mm



FIGURE 8. Transverse crack, CFS thickness 4mm

Verification of Shear Connector Capacity

After the test for investigating the shear connectors, all specimens were dismantled. It was observed that the shear connector had no rotation and deformation. The yielding is not appear around the bolts. This presented that the shear connector can provide composite action for transferring the longitudinal shear force without any failure occurring. The failure is less likely because of the crushing of concrete.

TEST RESULTS ANALYSIS

The aim of the flexural bending test was to evaluate the CFS-concrete composite beams performance. The obtained results are summarized in Table 4. The specimen's results were applied for parametric study.

Parametric Study, CFS Thickness

For evaluating the effect of results different thickness in all specimens were tested. The comparison of CFS ultimate moments, obtained by using 2 mm, 3 mm, and 4 mm thick and M_u , shown in Table 5. From Figure 11 it was observed that CFS-concrete composite floor specimens by increasing the CFS thickness experience capacities of ultimate moment, M_u increasing. The highest ultimate moment obtained at 4 mm thick then followed by 3 mm and 2 mm CFS thickness. The values increased from 15.9 % to 131%.

TABLE 4. Full-Scale beam testing results

Specimen	F_{ck} (MPa)	Ultimate Load, P_u (kN)	Deflection at P_u , exp. δ_u , exp. (mm)
FS1	33.4	188.5	137.6
FS2	33.4	191.1	136.2
FS3	33.4	194.4	133.7
FS4	35.8	346.2	122.1
FS5	35.8	361.3	110.9
FS6	35.8	364.1	92.4
FS7	36.2	399.7	124.4
FS8	36.2	408.8	116.4
FS9	36.2	413.3	112.7
FS10	34.1	440.6	49.7
FS11	32.6	472.1	54.9
FS12	32.6	438.5	49.6
FS13	35.3	466.1	56.9

TABLE 5. Ultimate strength of composite beams with different thickness of CFS

Specimen	CFS Thickness (mm)	Ultimate Moment, $M_{u,exp}$ (kNm)	$M_{u,exp}$ Increment (%)		Load, at first crack (kN)
FS1	2	131.9	-	-	95.2
FS2	2	133.7	FS1 vs FS2 = 1.4	-	102.4
FS3	2	136	FS1 vs FS3 = 3.1.	FS2 vs FS3 = 1.7	128.2
FS4	3	242.3	-	-	145.4
FS5	3	252.9	FS4 vs FS5 = 4.3	-	152.3
FS6	3	254.8	FS4 vs FS6 = 5.2	FS5 vs FS6 = 0.8	161.7
FS7	4	279.7	-	-	164.2
FS8	4	286.1	FS7 vs FS8 = 2.3	-	171.4
FS9	4	289.3	FS7 vs FS9 = 3.4	FS8 vs FS9 = 1.1	184.1
FS10	2.3	308.42	-	-	191.2
FS11	2.3	330.47	FS10 vs FS11 = 7.1	FS13 vs FS11 = 1.2	194.3
FS12	2.3	306.95	FS12 vs FS10 = 0.4	FS12 vs FS11 = 7.6	195.1
FS13	2.3	326.27	FS10 vs FS13 = 5.7	FS12 vs FS13 = 6.2	197.6

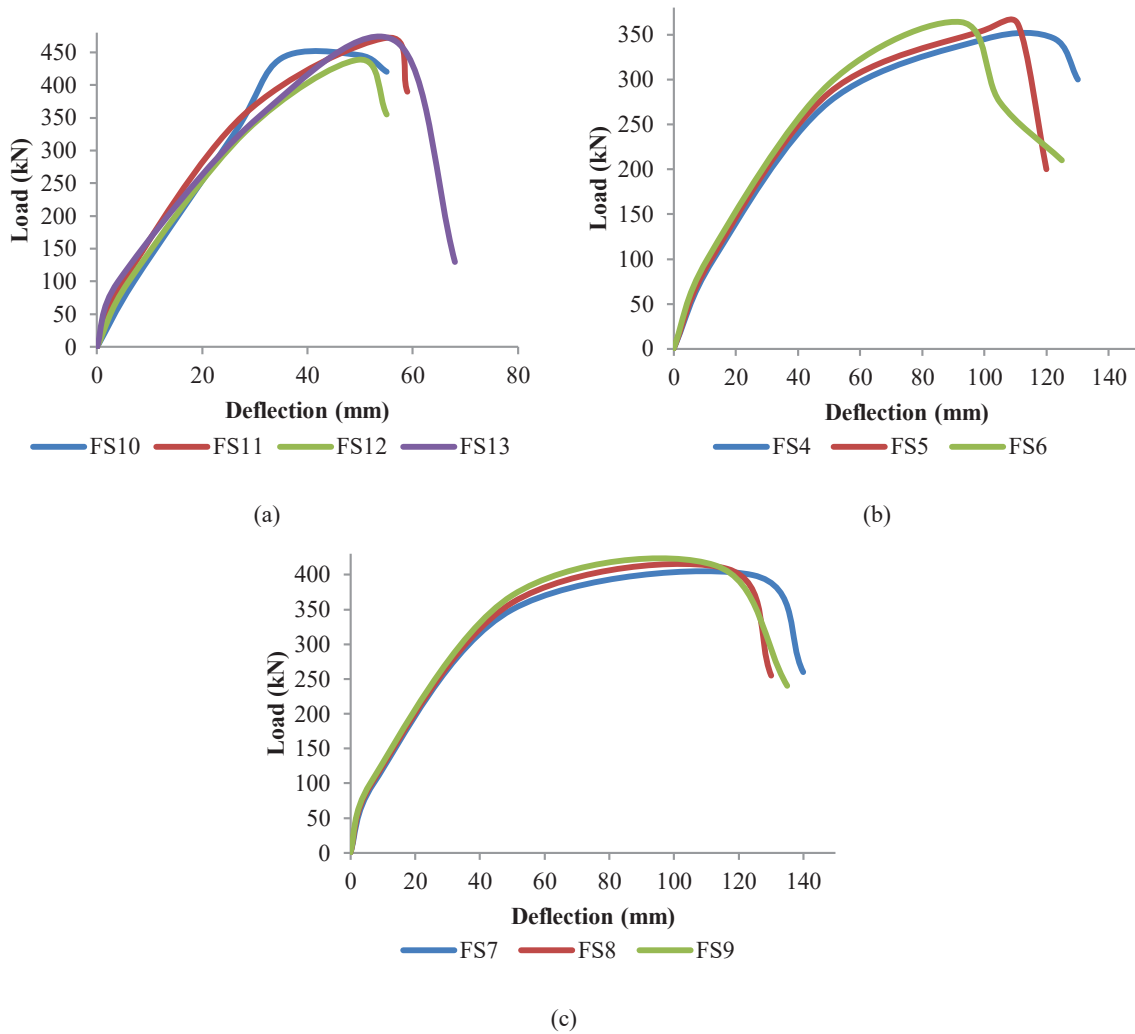


FIGURE 9. Effect of CFS thickness on load-deflection response; (a) thickness 2,3 mm; (b) thickness 3 mm; (c) thickness 4 mm

EXPERIMENTAL AND PREDICTED RESULTS

Ultimate moment capacities obtained results theoretically are compared with experimental outcomes as shown in Table 6. The resistance of tested sections is showed by applying plastic analysis. With the assumption of the strains across the section are enough high which CFS stresses are at their yield values level through the section and that the ferrocement has in its compression strength level. Plastic stress blocks are rectangular, different with elastic stress blocks that are triangular. Ferrocement section is reinforced with multiple reinforcement layers, it experiences a very ductile performance and behave as a perfectly plastic material with various properties in compression and intension.

Based on the plastic analysis results, the ferrocement CFS composite beams ultimate strength capacity can be properly evaluated by applying basic equilibrium approaches and the constitutive laws explained by standard tests and Euro codes regarding materials. The plastic analysis results comparison is shown in Table 6. The experimental to predicted plastic ultimate moment ratios from 0.93 to 1.27.

TABLE 6. Comparison of experimental data and theoretical analysis

Specimen	Test results	Theoretical analysis	Strength ratio
	Ultimate Moment, $M_{u,exp}$ (kNm)	Ultimate Moment, $M_{u,theo}$ (kNm)	
FS1	131.9	142.2	0.93
FS2	133.7	142.2	0.94
FS3	136	142.2	0.96
FS4	242.3	201.4	1.20
FS5	252.9	201.4	1.26
FS6	254.8	201.4	1.27
FS7	279.7	263.2	1.06
FS8	286.1	263.2	1.09
FS9	289.3	263.2	1.10
FS10	308.42	285.5	1.08
FS11	330.47	305.9	1.08
FS12	306.95	292.3	1.05
FS13	326.27	310.7	1.05

CONCLUSIONS

From this experimental work, can be concluded as follow:

1. In all specimens cracking pattern do not show high difference. Almost they were first formed under the loading positions because of the compressive stress concentration. CFS with 3 and 4 mm thickness, failed because of the concrete crushing. First crack formed under the tip of loading. Though, the mechanism of failure was different for different specimens. Sudden fracture of CFS was experienced.
2. A similar failure mode was experienced with the transverse cracks formation in the ferrocement in specimens with CFS thickness of 2 mm, as well as the channel sections tension yielding in the maximum bending moment region.
3. Transfer of longitudinal shear force due to composite action without failure were provided due to sufficient strength of shear connectors.
4. Strength capacity of specimens were experienced due to applying more layers of wire mesh of 6.
5. Specimens with CFS thickness of 4 mm carry 83.7% to 113.9% more ultimate moment in compare with specimens with CFS thickness of 2 and 3 mm respectively.
6. According to the plastic analysis results, the concrete cold formed composite beams ultimate strength capacity can be properly calculated by applying basic equilibrium approaches and the constitutive laws agreed by Euro codes and standard tests in the materials.
7. The results of plastic analysis in ultimate loads are closer to the experimental analysis outcomes, therefore it could be applied to design concrete CFS composite beams.

The most important contribution of this research is for the performance improvement of light-weight composite floor system. It proposes effective novel built-up sections of cold-formed steel (CFS) floor systems which act competitively with concrete slab to offer an alternative for roofs and floors of buildings.

ACKNOWLEDGEMENT

This study was graciously under construction research centre of UTM supporting and also with Structure and Construction Research Laboratory (SCRL), Faculty of Engineering, Sriwijaya University under the supervision of Prof. Dr. Ir. Anis Saggaff. The authors remain indebted for the support and collaboration given by both UTM-CRC and Sriwijaya University.

REFERENCE

1. R. M. Lawson, Slab and Beams with Steel Decking, the Steel Construction Institute Publication P055 Silwood Park Ascot, Berkshire SLS 7QN, UK, 1989.
2. W.K. Yu, K. F. Chung, M. F. Wong, [Journal of constructional steel research](#) **61**(9), 1332-1352 (2005).
3. J. M. Irwan, A. H. Hanizah, I. Azmi, [Journal of Constructional Steel Research](#) **65**, 2087–98 (2009)
4. S. N. Shaari, E. Ismail, *Promoting the use of industrialised building systems and modular coordination in the Malaysian construction industry* (Board of Engineers Malaysia, Bulletin Ingenieur, Malaysia, 2003), p.6–8.
5. A. E. Naaman, *Ferrocement and Laminated Cementitious Composites*, Techno Press 3000, (An Arbor, Michigan, USA, 2000).
6. Y. C. Wong, *Journal of Constructional Steel Research* **24**(10), 1159-1165 (1998).
7. J. Y. Richard, J. Y. Yiching, M. T. Lai **123**(6), 765-771 (1997).
8. M. Azimi, M. Ponraj, A. Bagherpourhamedani, M. M. Tahir, S. M. S. A. Razak, O. P. Pheng, [Jurnal Teknologi](#) **77**(16), 59–66 (2015).
9. M. Azimi, A. B. Adnan, M. M. Tahir, A. R. B. MohdSam, S. M. B. S. A. Razak, *Latin American Journal of Solids and Structures, an ABCM Journal* **12**(4), 787–807 (2015).
10. M. Azimi, A. Bagherpourhamedani, M. M. Tahir, A. R. B. M. Sam, C. K. Ma, [Journal of Advances in Structural Engineering](#) **19**(15), 730–745 (2016)
11. M. Azimi, A. B. Adnan, M. H. Osman, A. R. B. M. Sam, I. Faridmehr, R. Hodjati, [American Journal of Civil Engineering and Architecture](#) **2**(1), 42-52 (2014).
12. M. Azimi, A. B. Adnan, A. R. B. M. Sam, M. M. Tahir, I. Faridmehr, R. Hodjati, *The Scientific World Journal*, Article ID 802605, 12 pages, (2014).
13. T. M. Alhajri, M. M Tahir, M. Azimi, J. Mirza, M. M. Lawan, K. K. Alenezi, M. B. Ragaee, [Journal of Thin-Walled Structures](#) **102**, 18–29 (2016).
14. C. K. Ma, A. Z. Awang, R. Garcia, W. Omar, K. Pilakoutas, M. Azimi, *Journal of Structures*, Elsevier, **7**, 25-32 (2016).
15. C. K. Ma, A. Z. Awang, W. Omar, M. Liang, S. W. Jaw, M. Azimi, *Journal of Structural Concrete*, **1-25** (2016).
16. ASTM C39/C 39M-04. Standard test method for compressive strength of cylindrical concrete specimens. Annual Book of ASTM standards, 2004, vol. **4.02**.
17. ASTM C496/C496M-04. Standard test method for splitting tensile strength of cylindrical concrete specimens. Annual Book of ASTM standards, 2004. vol. **4.02**.
18. ASTM A370-03a. Standard test methods and definitions for mechanical testing of steel products. Annual book of ASTM standards, 2004, vol. **01.04**.